Talanta 99 (2012) 574–579

Contents lists available at SciVerse ScienceDirect

Talanta

journal homepage: www.elsevier.com/locate/talanta

Thiolated DAB dendrimer/ZnSe nanoparticles for C-reactive protein recognition in human serum

M. Algarra [a,*], B.B. Campos [b], D. Gomes [b], B. Alonso [c], C.M. Casado [c], M.M. Arrebola [d], M.J. Diez de los Rios [d], M.E. Herrera-Gutiérrez [e], G. Seller-Pérez [e], J.C.G. Esteves da Silva [b]

[a] Centro de Geología, Departamento de Geociências, Ambiente e Ordenamento do Território do Porto, Faculdade de Ciências da Universidade do Porto, Porto, Portugal
[b] Centro de Investigação em Química, Departamento de Química e Bioquímica, Faculdade de Ciências da Universidade do Porto, Porto, Portugal
[c] Departamento de Química Inorgánica, Universidad Autónoma de Madrid, Cantoblanco, 28049 Madrid, Spain
[d] Laboratorio de Urgencias, Servicio de Análisis Clínicos, Complejo Hospitalario Carlos Haya, Málaga, Spain
[e] Servicio de Cuidados Críticos y Urgencias, Complejo Hospitalario Carlos Haya, Málaga, Spain

ARTICLE INFO

Article history:
Received 28 March 2012
Received in revised form
8 June 2012
Accepted 15 June 2012
Available online 20 June 2012

Keywords:
ZnSe quantum dots
Dendrimers
O-phosphorylethanolamine
C-reactive protein
Serum samples

ABSTRACT

A nanocomposite obtained by a thiol DAB-dendrimer (generation 5), coated with fluorescent ZnSe quantum dots, was successfully synthesized for the selective recognition of C-reactive protein. The procedure presented was carried out by a novel, cheap and non-toxic bottom up synthesis. The nanocomposite showed an excitation at 180 nm, with two emission bands at 411 and 465 nm, with a full-width at half-maximum of 336 nm. The Stokes shift was influenced by the presence of coating molecules and the intensity was dependent on pH due to the presence of a charge transfer process. The transmission electron microscopy images demonstrated that the spherical nanoparticles obtained displayed a regular shape of 30 nm size. The fluorescence intensity was markedly quenched by the presence of C-reactive protein, with a dynamic Stern–Volmer constant of 0.036 M^{-1}. The quenching profile shows that about 51% of the ZnSe QDs are located in the external layer of the thiol dendrimer accessible to the quencher. The precision of the method obtained as relative standard deviation was 3.76% (4 mg L^{-1}, $n=3$). This water soluble fluorescent nanocomposite showed a set of favorable properties to be used as a sensor for the C-reactive protein in serum samples, at concentrations of risk levels.

1. Introduction

Due to their narrow and intensive emission spectra, continuous absorption band, high chemical and photobleaching stability, processability and surface functionality, much interest has arisen in the preparation of semiconductor quantum dots (QDs), as emerging probe for chemical sensing. There is a wide range of very efficient light emitting QDs, which can be synthesized both in organic or in aqueous solutions [1–9]. It is well known that the fluorescence efficiency of the QDs is sensitive to the presence and nature of ligands on their surface [10]; therefore it is expected that QDs, used as sensing probe, can be developed due to the fluorescence changes induced by the molecular recognition on their surface.

Since the first reports using modified core–shell QDs, as fluorescence labels to stain biological samples, inorganic luminescent QDs have attracted considerable attention as novel fluorescent indicators of different biological processes and bioanalyses [11,12]. Practical uses of QDs coated with different organic ligands were developed as chemical sensors, such as L-cysteine and thioglycerol to determine metal ions in aqueous media [13], mercaptoacetic acid for Hg(II) [14], triethanolamine [15], and macromolecules such as calixarene for Hg(II) and Se analyses [16,17], and DAB dendrimers for Hg(II) [18] and organic nitrocompounds [19,20].

Dendrimers have unique molecular structures and their properties make them attractive molecules in nanotechnology. They are well defined hyperbranched polymers with a high density of functional groups and constitute attractive scaffolds as multivalent natural ligands [21–23]. Polyamidoamine (PAMAM) dendrimers are multifunctional water-soluble macromolecules that are capable of bearing dyes [24], antibodies [25], proteins [26] and amino acids [27]. Moreover thiolated PAMAM and DAB dendrimers were used as protein transfer [28] and Cd(II) and Pb(II) sensors [29].

In this work, the novel synthesis procedure of a thiol polypropylenimine dendrimer, generation 5, coated with ZnSe–PEA QDs in aqueous media (S-DAB–ZnSe–PEA QDs) is described. The

* Corresponding author. Tel.: +351 220 402 568; fax: +351 220 402 659.
E-mail address: magonzal@fc.up.pt (M. Algarra).

0039-9140/$ - see front matter © 2012 Elsevier B.V. All rights reserved.
http://dx.doi.org/10.1016/j.talanta.2012.06.037

quenching of the nanocomposite fluorescence caused by C-reactive protein (CRP) was investigated and the sensing capabilities of this probe for CRP quantification in serum samples were assessed. The determination of CRP levels can provide a rapid diagnosis of infections and inflammation in patients.

2. Materials and experimental methods

2.1. Chemical and reagents

Zinc nitrate (99.9%, $(Zn(NO_3)_2 \cdot 4H_2O)$, selenium powder (Se, 99.99%), sodium borohydride ($NaBH_4$, $\geq 96\%$), 3-mercaptopropionic acid (MPA, 99%), triethylamine (TEA), C reactive protein (CRP) and *O*-phosphorylethanolamine (PEA) were purchased from Sigma-Aldrich Química S.A. (Spain) and used without further purification. Thiolated polypropylenimine dendrimer DAB-AM-(64) generation 5 (S-DAB) was synthesized at Universidad Autónoma de Madrid (Spain), as reported previously [30].

The serum samples were obtained from patients from the Carlos Haya Hospital (Málaga, Spain) according to their own procedure and stored at $-20\ ^{\circ}C$ until prior analysis. The sample concentrations were determined by means of the CRP extended range (rCRP) method, an immune-turbidimetric assay. The analytical measurement range is: 0.5–250 mg L^{-1} with an analytical sensitivity of 0.5 mg L^{-1} and for the lowest concentration of the CRP that can be distinguished from zero, the functional sensitivity as relative standard deviation (RSD) was obtained to be <20; for 1.1 mg L^{-1} RSD = 17.7% was obtained.

2.2. Synthesis of S-DAB–ZnSe–PEA QDs

To prepare the S-DAB–ZnSe–PEA QDs, 10 mg of S-DAB dendrimer was stirred in deionized H_2O (50 mL) for 72 h. Then, 7 mg of $Zn(NO_3)_2$ was added and left under stirring for 24 h to ensure the total complexation of Zn^{2+} with S-DAB dendrimer. MPA (17.6 μL) was then added to this solution and stirred for 24 h. After this, TEA was used to adjust the pH to 12 and 200 μL of Se solution (as NaHSe) was added [20]. Finally, the addition of PEA (14.3 mg) resulted in S-DAB–ZnSe–PEA QDs after 24 h. All the synthesis procedures were carried out at room temperature under N_2 flow. Fig. 1 represents the molecular system obtained by a bottom-up strategy.

2.3. Instrumentation

A UV–vis spectrophotometer (Hewlett-Packard HP8452A diode array) and a photoluminescence spectrophotometer (Horiba Jovin Yvon Fluoromax 4 TCSPC) were used to characterize S-DAB–ZnSe–PEA QDs. UV–vis absorption spectrum of QDs was scanned in the wavelength range of 180–400 nm. The fluorescence measurements were carried out between 300 and 740 nm, using an integration time of 0.1 s and a slit width of 5 nm for excitation and emission respectively. Samples were contained in a 1-cm path length quartz cuvette. Transmission electron microscopy (TEM) and energy dispersive X-ray (EDAX) studies of S-DAB–ZnSe–PEA QDs were performed on a Philips CM-200 by evaporating one drop on carbon coated cooper. The size and zeta potential (ζ) of S-DAB–ZnSe–PEA QDs were determined using a

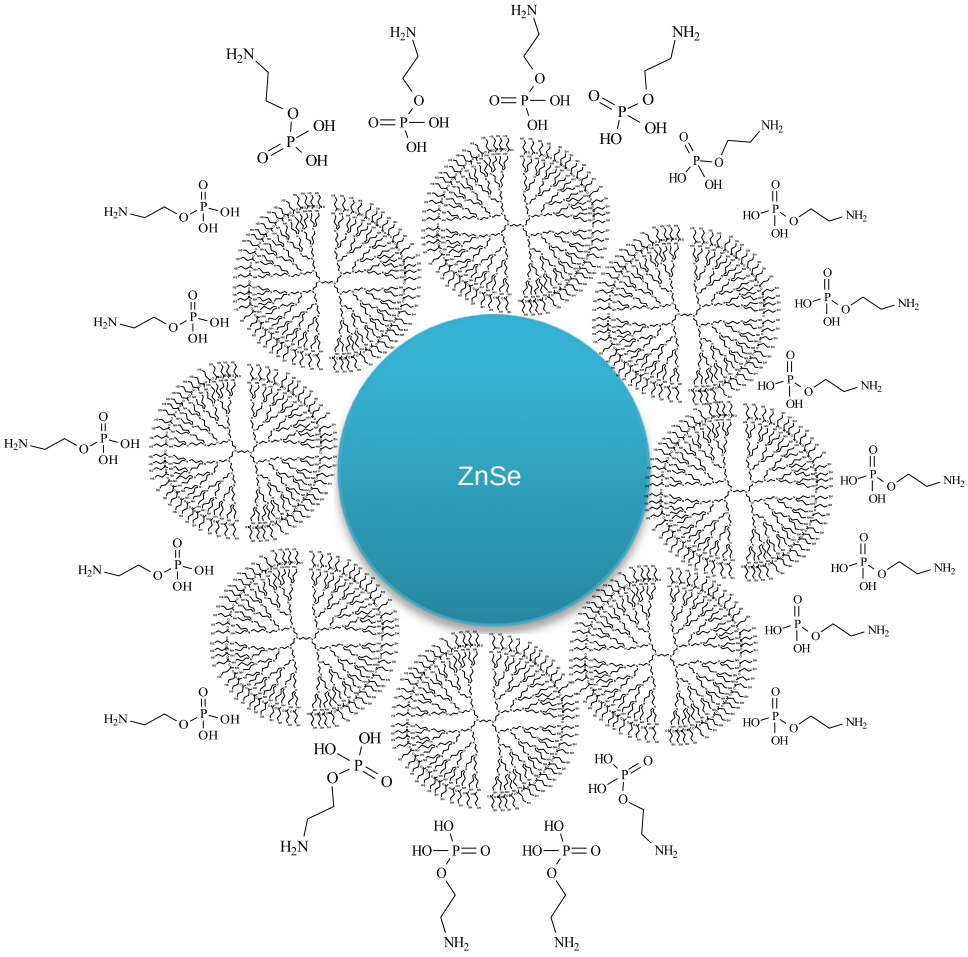

Fig. 1. Schematic representation of the S-DAB–ZnSe–PEA QDs system.

Zetasizer Nano ZS (Malvern Instruments, UK) equipped with a 4 mW HeNe laser operating at $\lambda=633$ nm. All samples were measured at scattering angles of 173° (for size) and 13° (ζ) that were average of three tests. Size measurements, using dynamic light scattering (DLS), were performed at 25 °C in a polystyrene cell (ZEN0040). The ζ measurements were also performed at 25 °C in polycarbonate folded capillary cells, incorporated with gold plated electrodes (DTS1060C) with deionized H_2O as the dispersion medium. Both size and ζ were automatically obtained by the software, using the Stokes–Einstein and the Henry equations, with the Smoluchowski approximation.

2.4. Procedure for sensing CRP by S-DAB–ZnSe–PEA QDs

Aliquots of CRP samples were placed in a 5 mL calibrated flask with 2 mL of S-DAB–ZnSe–PEA QDs, which were obtained as described in Section 2.2, and, filled with $CaCl_2$ (0.01 M) to ensure a pH of 7 and avoid the denaturalization of the CRP. The fluorescence spectra were recorded between 300 and 740 nm ($\lambda_{ex}=180$ nm). The serum samples were analyzed using the following procedure: aliquots of serum (500 μL) with concentrations between 0.5 and 100 mg L^{-1} were placed in 5 mL calibrated flasks containing 2 mL of S-DAB–ZnSe–PEA QDs and, filled with $CaCl_2$ (0.1 M) at pH 7 and, the fluorescence measurements were recorded as described above.

2.5. Fluorescence data analysis

In this study collisional quenching of fluorescence by CRP was described using the Stern–Volmer equation:

$$\mathbf{I}_o/\mathbf{I} = 1 + K_D[\mathbf{CRP}] \quad (1)$$

where $\mathbf{I}_o$ is the fluorescence intensity without CRP, $\mathbf{I}$ is the fluorescence intensity observed in the presence of CRP and K_D is the dynamic (collisional) Stern–Volmer constant. The quenching was also described by a modified Stern–Volmer equation accounting for a fractional accessibility to quenchers:

$$\mathbf{I}_o/\mathbf{DI} = 1/(f_a K_a[\mathbf{CRP}] + 1/f_a \quad (2)$$

where $\Delta\mathbf{I}=(\mathbf{I}_o-\mathbf{I})$, f_a is the fraction of initial fluorescence that is accessible to quencher and K_a is the Stern–Volmer quenching constant of the accessible fraction [31].

3. Results and discussion

3.1. Synthesis of S-DAB–ZnSe–PEA QDs

The synthesis procedure was significantly different to those previously reported in the literature [32,33]. Fig. 2 shows the room temperature fluorescence spectra of the S-DAB–ZnSe QDs with PEA, excited at 180 nm (UV–vis spectrum, see inset in Fig. 2), which is the selective chemical sensor for CRP, and this was compared with the raw ZnSe QDs. The coating effect of S-DAB is markedly red shifted to 465 nm ($\Delta\lambda=51$ nm), because when the S-DAB dendrimer is not present in the structure, the most intense band is centered at 410 nm. The anchorages of S-DAB to the surface of ZnSe QDs provide stabilization, in terms of band gap of 0.32 eV to the QDs. Moreover, the S-DAB dendrimers act as protecting agents from the surrounding environment, increasing the fluorescence efficiency compared with the raw ZnSe QDs. As can be seen, the QDs coated with PEA exhibited a red shift and a relative increase of intensity.

The presence of MPA is an important key in the synthesis procedure; no fluorescence emission is obtained if MPA is not involved. The emission full-width at half-maximum (FWHM) is

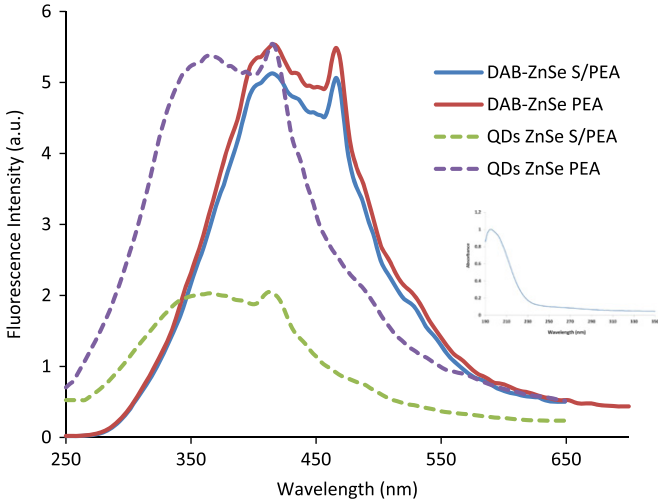

Fig. 2. Emission spectra of S-DAB–ZnSe–PEA QDs (red) compared with the raw ZnSe (gray); ZnSe–PEA (blue), and S-DAB–ZnSe QDs (black), synthesized at pH 12 and excited at 180 nm. (For interpretation of the references to color in this figure legend, the reader is referred to the web version of this article.)

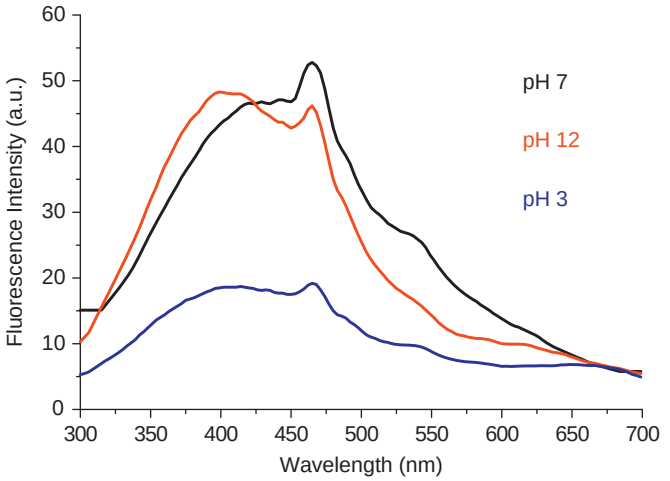

Fig. 3. Effect of pH in the emission bands of S-DAB–ZnSe–PEA QDs.

336 nm, a relatively high value when compared with the typical narrower emission bands of QDs, but similar to those obtained recently [32,33]. This high FWHM suggests that S-DAB–ZnSe–PEA QDs show a high degree of heterogeneity, probably because they are bounded to different chemical environments. The presence of two bands is noticeable, which can be explained as a consequence of the change of the quantum confinement of the QDs, explained by the formation of ZnSe wurzite structure [32].

3.2. Effect of pH and ionic strength

pH is one of the main variables that affect the fluorescence of QDs. Therefore the effects of pH on the maximum and the intensity of the fluorescence over S-DAB–ZnSe–PEA QDs were studied. It was found that the signals do not suffer any shift in the maximums of fluorescence. Significant changes in both bands were observed when the pH is changed. The pH of 12 induces and increases emission intensity at 391 nm while the band at 465 nm decreases. However at pH 3 and 7 the opposite effect is observed (Fig. 3). This effect is more pronounced when the ZnSe–PEA QDs are diluted at pH 12. This change in the band shape can be explained on the basis of the change of the polarity and H^+ donor ability in the surrounding

environment of the nanoparticles. On the other hand, taking into account that at this pH the precipitation of $Zn(OH)_2$ should occur, it is noteworthy that fluorescence does not decrease, which may be explained considering that S-DAB dendrimer establishes a stable environment from the medium.

The presence of amino groups (–NH) in the inner structure of S-DAB also affects the non-radiative decay rate, decreasing it and increasing the transitions to the ground state of the ZnSe QDs [34], when the pH is increased thereby increasing the polarity of the medium, which in turn induce the de-protonation of –NH, since some of the electronic transitions involve charge transfer, such as the singlet charge transfer transitions which is accelerated by the change of polarity. The ζ of the sensor presents a negative charge with −46.6 mV (Supplementary information Fig. SI 1). This value is concordant with the size values because low ζ value does not prevent the particles from aggregating together and flocculating. Other reason for a negative ζ is the basicity of the medium where the system was synthesized.

To investigate the effect of ionic strength on fluorescence, different solutions at pH 7 with increasing concentration of KCl were studied, containing 0.002, 0.02, 0.2, 0.4, 1 and 1.5 M of KCl. Results emphasize that fluorescence decreases when salt concentration is increased. It has been demonstrated that as the positive ion cloud around the complex system increases, it occupies the available binding sites on the surface and reduces the possibility for protection. A decrease in fluorescence intensity of the S-DAB–ZnSe–PEA QDs may also be ascribed to the deactivation process by the surrounding H_2O molecules. It is evident that the percentage of fluorescence hypo-chromicity is moderate, from lower to higher ionic strength around 30%, as illustrated in supplementary information (Fig. SI 2).

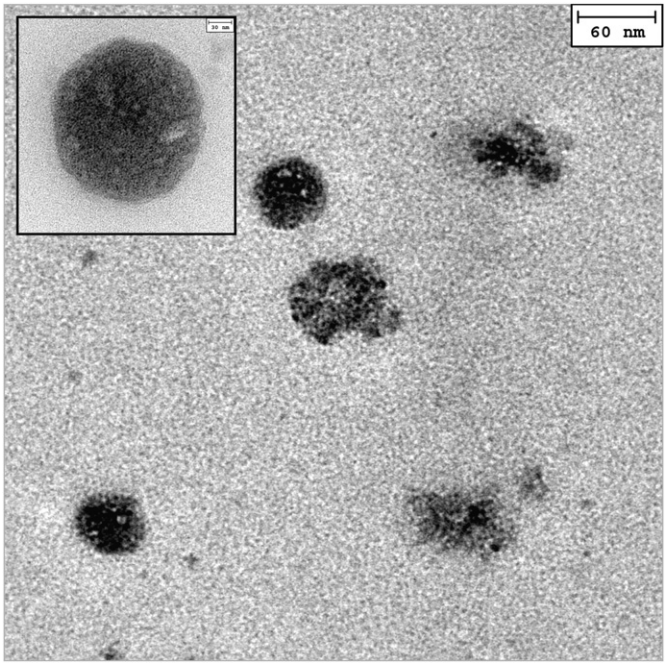

Fig. 4. TEM image of S-DAB–ZnSe–PEA QDs nanoparticles. Inset of a TEM image showing the spherical shape (scale bar represents 30 nm).

3.3. TEM analysis

Fig. 4 shows the TEM image of S-DAB–ZnSe–PEA QDs. The size was about 40 nm, and showed a regular spherical shape (inset of Fig. 4). This shows a pattern of association of a few particles, which is possibly due to conjugation of QDs with dendrimers which is not observed in case of ZnSe QDs alone. Some particles agglomerated also due to dipolar interactions between dendrimers in aqueous medium. The EDAX analysis (not shown here) demonstrated the general composition of the nanoparticles studied, where Se, Zn and S are the predominant elements. In the synthesis of the aqueous S-DAB–ZnSe–PEA QDs nanoparticles, MPA was used as the coating molecule. The thiol group (–SH) of the MPA attached to the Zn^{2+} cation on the particle surface and the carboxyl group ($-COO^-$) on the other end of the MPA was fully charged at high pH values. As a result, the QDs were stabilized and dispersed from each other due to the electrostatic repulsion.

These results prove the formation of agglomerates by S-DAB dendrimer, which have a large range of size values that varies from 50.75 nm to 612.4 nm. Two populations of nanoparticles with mean sizes of 317.4 and 109 nm show the higher scattering intensity percentage (Fig. 5 and supplementary information Fig. SI 3). The surrounding medium influences the physical and chemical behavior of the dendrimer, which can adapt, individually, a close or open conformation and, collectively, a low or high agglomeration, depending on the electric charge inside and on the surface of the dendrimer, being very sensitive to pH and ionic strength changes. The size of the nanocomposites is larger than that observed by TEM image. It is reasonable because TEM and DLS show different morphologies in a solid or swollen state.

3.4. Sensing to CRP by S-DAB–ZnSe–PEA QDs

The effect of CRP on the fluorescence emission of the S-DAB–ZnSe–PEA QDs is shown in Fig. 6a. The fluorescence intensity is

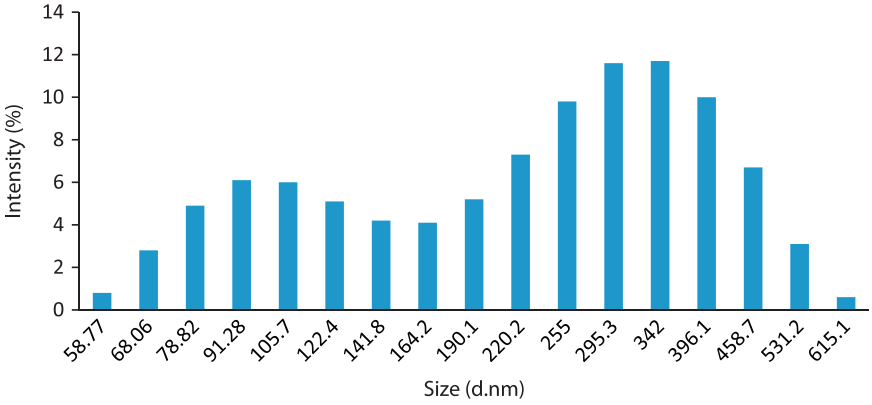

Fig. 5. S-DAB–ZnSe–PEA QDs size (mean diameter) assessed by DLS. Results are expressed as the mean obtained from three independent experiments.

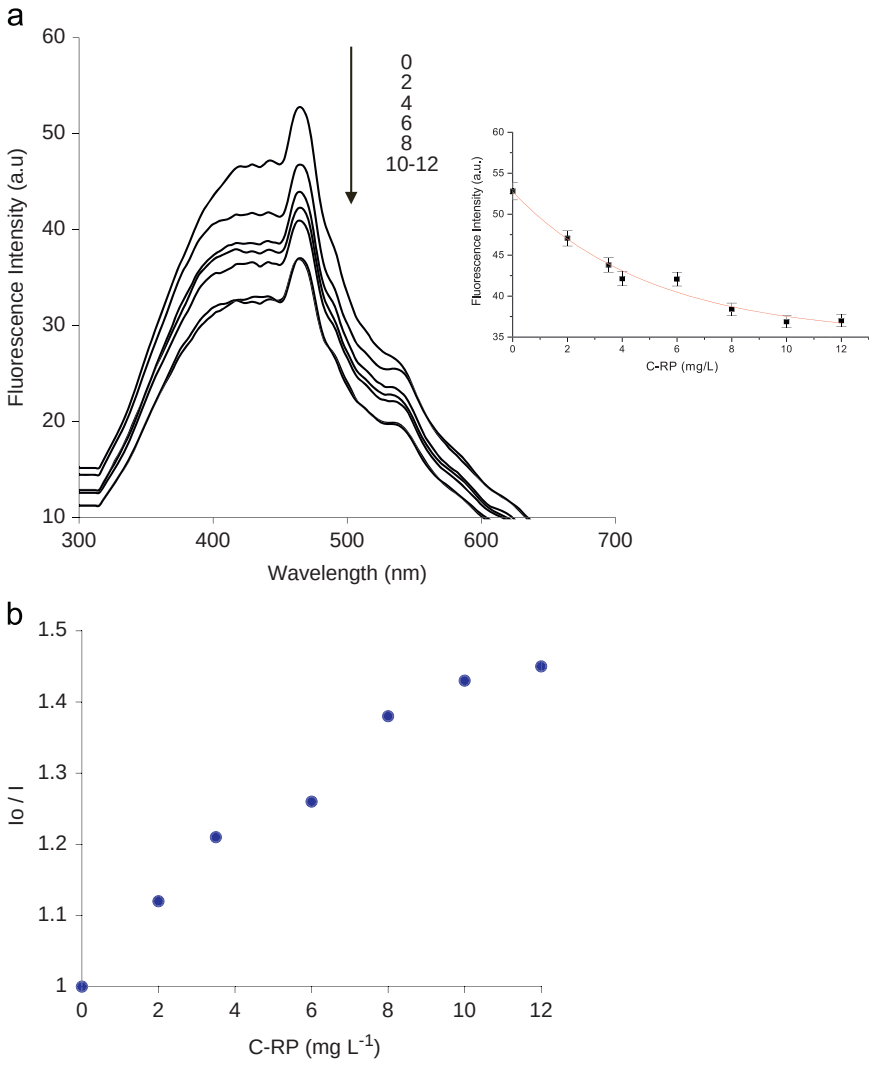

Fig. 6. (a) Effect of CRP in fluorescence of S-DAB–ZnSe–PEA QDs and (b) Stern–Volmer representation of S-DAB–ZnSe–PEA QDs.

significantly quenched by the addition of CRP. Quenching effect by CRP on the fluorescence emission of the S-DAB–ZnSe–PEA is found to be concentration dependent. Therefore, this system can be used for the development of a sensitive and selective method for CRP sensor. The analysis of Fig. 6a shows that a linear trend is observed in the CRP concentration range between 0 and 10 mg L^{-1}. The linearization equation derived from the experimental data (deviation under parenthesis) with correlation coefficient >0.99; $n=3$) is as follows:

$$\mathbf{I} = -2 \times 10^{-8}(2.3)\mathbf{Log}[\mathbf{CRP}] + 5 \times 10^{-8} \quad (3)$$

where **I** is the fluorescence intensity of the S-DAB–ZnSe–PEA in the presence of CRP and Log[**CRP**], expressed in mg L^{-1}. The precision of the method obtained (as RSD) for 4 mg L^{-1} ($n=3$) was 3.76%.

A detailed analysis of the Stern–Volmer plots shows the existence of a slightly downward curvature. This observation is supported by the calculated intercept, 1.94 (6), which is significantly higher than the expected unity, and suggests that not all the fluorophores dispersed on the dendrimer structure are accessible to the quencher (CRP) [31]. To assess this hypotheses a modified Stern–Volmer plot was obtained (Fig. 6b) and, with this model, a better linear fitting of the quenching profiles as function of CRP concentration is achieved. From the modified Stern–Volmer plots a Stern–Volmer constant of 0.036 (6) M^{-1} is calculated and the percentage of fluorophores accessible to the quencher is about 51%. This result shows that about 49% of the S-DAB–ZnSe–PEA QDs (fluorophores) are located in the inner layers of the dendrimer while about 51% are located in the external layer of the thiol dendrimer. The quenching effect of CRP on the fluorescence emission of S-DAB–ZnSe–PEA, was recently published in the determination of

Table 1
Results obtained with S-DAB–ZnSe–PEA QDs in serum samples[a].

CRP (mg L^{-1})	CRP found (mg L^{-1})	CRP labeled[b] (mg L^{-1})	CRP found (mg L^{-1})	Error (%)
0.5	0.61 (1.32)	5	6.10	22.0
1	1.07 (1.78)	10	11.70	7.0
2	2.13 (2.43)	20	22.50	6.5
4	4.36 (3.91)	40	43.60	9.0
6	6.35 (3.70)	60	66.50	5.8
8	8.96 (4.12)	80	89.60	12.0
10	12.33 (4.66)	10	12.30	23.0
10	13.89 (5.16)	100	138.90	38.9

[a] Average and standard deviation for $n=3$ (under parenthesis and referring to the last significant digit).
[b] The concentrations of the samples were determinated by means the CRP Extended Range (rCRP) method, an immune-turbidimetric assay.

CRP by means of CdSe–PEA QDs [35] and a fluorescent polymer coated with PEA [36].

3.5. Analysis of serum samples

In order to assess the potential of the S-DAB–ZnSe–PEA QDs based method for the analysis of CRP, real serum samples of sick or recently operated patients were tested. The results obtained, showed in Table 1 using S-DAB–ZnSe–PEA QDs, were acceptable in the risk concentrations of interest for clinical assay (1–8 mg L^{-1}) and moderate in the other level of concentrations studied. The results are compared with those obtained by the immnunoassay method used in hospital as a routine analysis.

4. Conclusions

A CRP sensing probe based on the quenching of the fluorescence of ZnSe–PEA QDs coated by S-DAB dendrimer was developed. The recognition polymeric system was constructed by a bottom-up strategy and, by changing the pH media, the behavior of the fluorescence emission bands was analyzed. The morphology and the reactive surface were characterized by the TEM, DLS and ζ techniques. At pH 7, the recognition of CRP by the S-DAB–ZnSe–PEA QDs sensor was successfully carried out in the level of risks concentrations. The RSD obtained substantially improved the values obtained by the immunoassay method for CRP used as a routine analysis in the hospital as reference. S-DAB dendrimer must be taken into account due to its great potential in the development of clinical sensing methodology.

Acknowledgments

The authors would like to thank Ciência 2007 (FCT program) and the Spanish Ministerio de Ciencia e Innovación (Project CTQ2009-12332-C02-01). Financial funds (FCT, Lisbon), Programa Operacional Temático Factores de Competitividade (COMPETE) and shared by FEDER funds Project PTDC/QUI/71001/2006) are acknowledged.

Appendix A. Supporting information

Supplementary data associated with this article can be found in the online version at http://dx.doi.org/10.1016/j.talanta.2012.06.037.

References

[1] L. Spanhel, M. Haase, H. Weller, A. Henglein, J. Am. Chem. Soc. 109 (1987) 5649.
[2] C.B. Murray, D.J. Norris, M.G. Bawendi, J. Am. Chem. Soc. 115 (1993) 8706.
[3] A.P. Alivisatos, J. Phys. Chem. 100 (1996) 13226.
[4] O.I. Micic, J. Sprague, Z. Lu, A.J. Nozik, Appl. Phys. Lett. 68 (1996) 3150.
[5] A. Rogach, S. Kershaw, M. Burt, M. Harrison, A. Kornowski, A. Eychmuller, H. Weller, Adv. Mater. 11 (1999) 552.
[6] Y.W. Cao, U. Banin, J. Am. Chem. Soc. 122 (2000) 9692.
[7] N. Gaponik, D.V. Talapin, A.L. Rogach, K. Hoppe, E.V. Shevchenko, A. Kornowski, A. Eychmuller, H. Weller, J. Phys. Chem. 106 (2002) 7177.
[8] B.L. Wehrenberg, C. Wang, P. Guyot-Sionnest, J. Phys. Chem. B 106 (2002) 10634.
[9] H. Du, C. Chen, R. Krishnan, T.D. Krauss, J.M. Harbold, F.W. Wise, M.G. Thomas, J. Silcox, Nano Lett. 2 (2002) 1321.
[10] C.J. Murphy, Anal. Chem. 74 (2002) 520A.
[11] M.J. Bruchez, M. Moronne, P. Gin, S. Weiss, A.P. Alivisatos, Science 281 (1998) 2013.
[12] W.C.W. Chan, S.M. Nie, Science 281 (1998) 2016.
[13] Y.F. Chen, Z. Rosenzweig, Anal. Chem. 74 (2002) 5132.
[14] M. Koneswaran, R. Narayanaswamy, Sensors Actuators B 139 (2009) 91.
[15] Z.B. Shang, Y. Wang, W.J. Jin, Talanta 78 (2009) 364.
[16] H. Li, W. Xiong, Y. Yan, J. Liu, H. Xu, X. Yang, Mater. Lett. 60 (2006) 703.
[17] H. Li, Y. Zhang, X. Wang, D. Xiong, Y. Bai, Mater. Lett. 61 (2007) 1474.
[18] B.B. Campos, M. Algarra, B. Alonso, C.M. Casado, J.C.G. Esteves da Silva, Analyst 134 (2009) 2447.
[19] B.B. Campos, M. Algarra, J.C.G. Esteves da Silva, J. Fluoresc. 20 (2010) 143.
[20] M. Algarra, B.B. Campos, M.S. Miranda, J.C.G. Esteves da Silva, Talanta 83 (2011) 1335.
[21] A.W. Bosman, H.M. Janssen, E.W. Meijer, Chem. Rev. 99 (1999) 1665.
[22] J.P. Mitchell, K.D. Roberts, J. Langley, F. Koentgen, J.N. Lambert, Bioorg. Med. Chem. Lett. 9 (1999) 2785.
[23] U. Boas, P.M.H. Heegard, Chem. Soc. Rev. 33 (2004) 43.
[24] D.A. Tomalia, A.M. Naylor, W.A. Goddard III, Angew. Chem. Int. Engl. 29 (1990) 138.
[25] K.K. Ong, A.L. Jenkins, R. Cheng, D.A. Tomalia, H.D. Durst, J.L. Jensen, P.A. Emanuel, C.R. Swim, R. Yin, Anal. Chim. Acta 444 (2001) 143.
[26] B. Pan, F. Gao, H. Gu, J. Colloid Interface Sci. 284 (2005) 1.
[27] M.F. Ottaviani, S. Jockusch, N.J. Turro, D.A. Tomalia, A. Barbon, Langmuir 20 (2000) 10238.
[28] A.C. Wisher, I. Bronstein, V. Chechik, Chem. Commun. (2006) 1637.
[29] M. Algarra, B.B. Campos, B. Alonso, M.S. Miranda, Á.M. Martínez, C.M. Casado, J.C.G. Esteves da Silva, Talanta 88 (2012) 403.
[30] S. Connolly, S.N. Rao, D. Fitzmaurice, J. Phys. Chem. B 104 (2000) 4765.
[31] J.R. Lakowicz, Principles of Fluorescence Spectroscopy, second ed., Plenum Press, New York, 1999. (p. 243).
[32] P. Kumar, K. Singh, J. Optoelect. Biomed. Mater. 1 (2009) 59.
[33] B.H. Kwon, H.S. Jang, H.S. Yoo, S.W. Kim, D.S. Kang, S. Maeng, D.S. Jang, H. Kima, D.Y. Jeon, J. Mater. Chem. 21 (2011) 12812.
[34] F.G. Sánchez, A.N. Díaz, M. Algarra, J. Lovillo, A. Aguilar, Spectrosc. Chim. Acta A 84 (2011) 88.
[35] K. Sreenivasan, V. Raj, P.R. Hari, Anal. Chim. Acta 592 (2007) 45.
[36] D. Gomes, M. Algarra, M.J. Diez de los Rios, M.M. Arrebola, M.E. Herrera Gutierrez, G. Seller-Perezd, J.C.G. Esteves da Silva, Talanta 93 (2012) 411.